Self-elongation and Nonlinear Intensification of Unstable Baroclinic Vortices

Georgi Sutyrin GSO/URI, USA

Self-elongation of Circular Compensated Vortices
Nonlinear Stabilization in Carousel Multipoles
Hamiltonian Elliptical Core Vortex Model
Self-intensification in Metastable Corotating States
Sharp Vorticity Gradients and Solid -body Rotation
Comparison with Eddies in the Northwest Corner

ejh2016, Grenoble, France

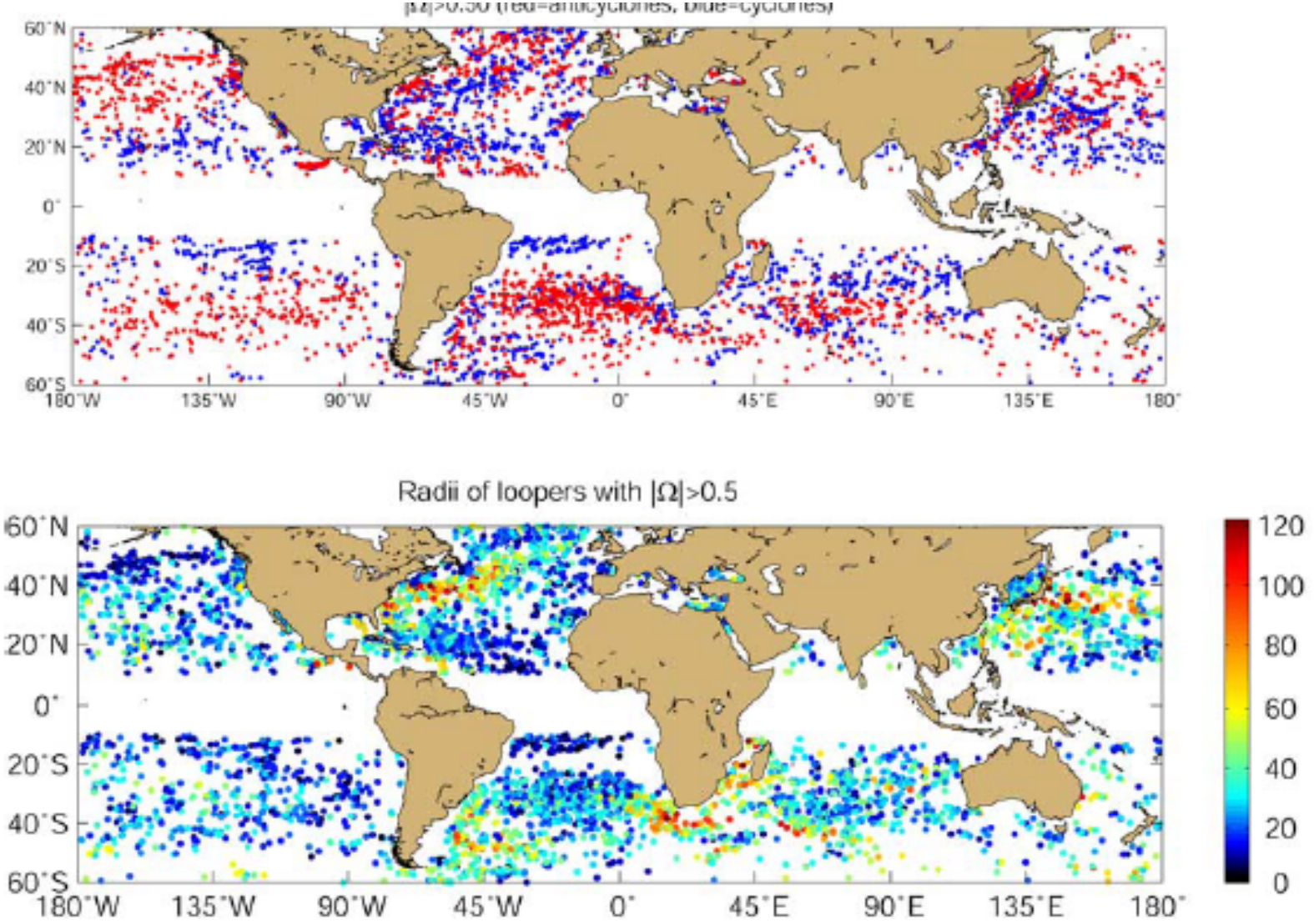

Figure 3. Distribution of individual trajectories with defined sense of rotation (spin values $|\Omega| > \Omega_c$). Each dot corresponds to the medial position of a trajectory segment of length $T_{seg} = 20$ days and $|\Omega| > \Omega_c = 0.5$ day^{-1}. Similar results are obtained for $T_{seg} = 40$ days and $\Omega_c = 0.4–0.6$ day^{-1} (not shown). (top) Distribution of polarity; cyclonic (blue) and anticyclonic (red). (bottom) Distribution of radial space scale $R = u_{rms}/\Omega$ (km).

The effect of ageostrophy on the stability of vortices in a two-layer ocean

E.S. Benilov *, J.D. Flanagan Ocean Modelling 23 (2008) 49–58

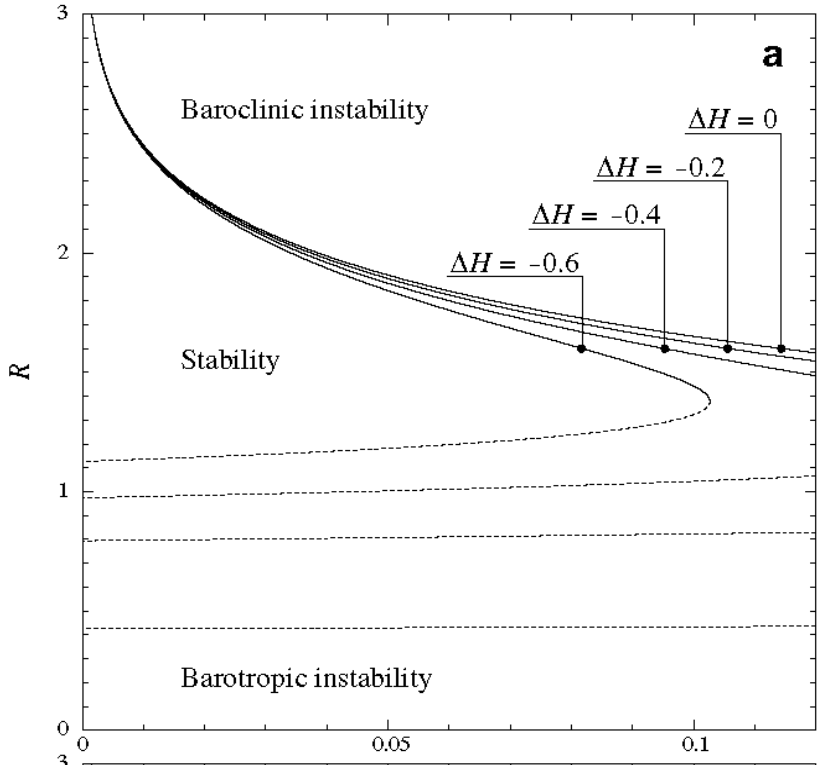

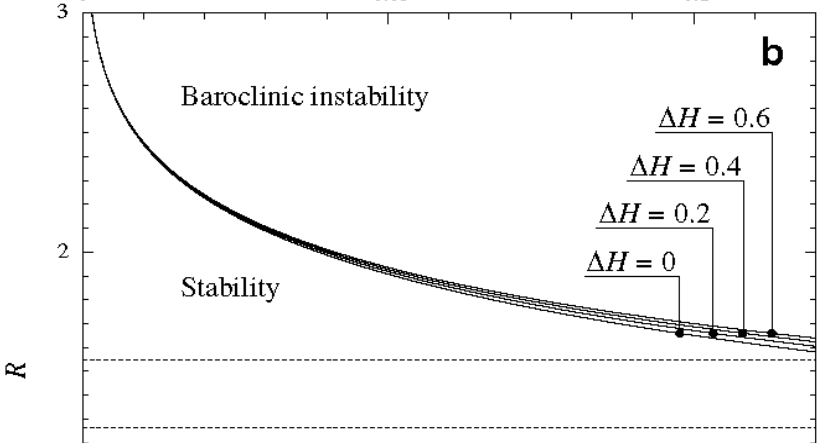

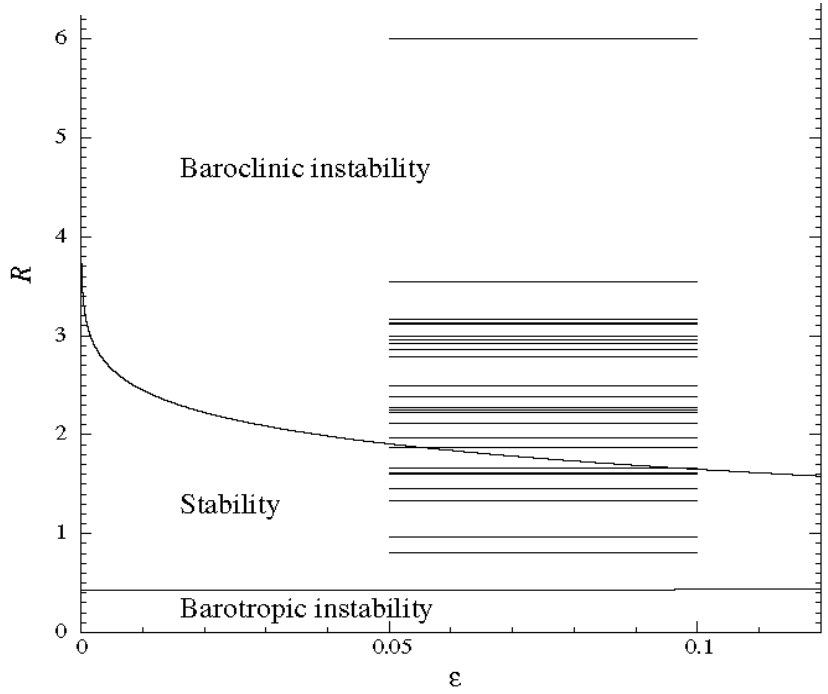

Fig. 6. The marginal stability curve for Gaussian quasigeostrophic ($\Delta H \to 0$) vortices, for the second azimuthal mode ($k = 2$). Horizontal segments show the parameters of rings catalogued in Olson (1991).

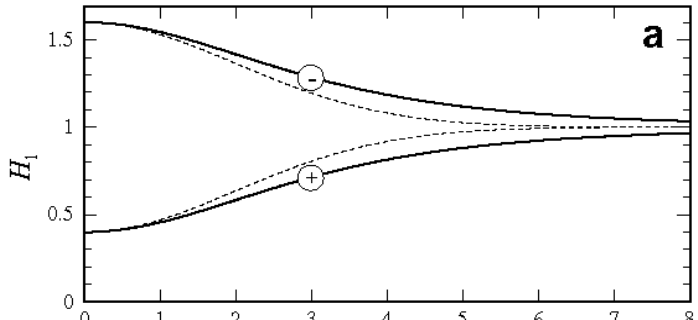

The most theoretical work on the linear and nonlinear stability of axisymmetric baroclinic vortices [*Ikeda*, 1981; *Flierl*, 1988; *Helfrich and Send*, 1988; *Carton and McWilliams*, 1989; *Ripa*, 1992; *Killworth et al.*, 1997; *Benilov et al.*, 1998; *Correard and Carton*, 1999; *Sokolovskiy and Verron*, 2000; *Baey and Carton*, 2002; *Benilov*, 2003, 2005; *Katsman et al.*, 2003] suggests that rings are expected to be unstable in a typical parameter range when their size is substantially larger than the baroclinic radius of deformation. For a two-layer ocean model, *Dewar and Killworth* [1995] have found stabilizing effect of a corotating circulation on a Gaussian vortex in the upper layer: even a relatively weak deep flow may stabilize the eddy. This effect has been later examined for other vortex shapes where a corotating deep flow would just reduce the growth rate with unsatisfactory conclusions: "the observed stability of cold rings remains a dynamical enigma" [*Dewar et al.*, 1999] or "in the end we are left with the puzzling result that realistic rings are quite unstable according to linear analysis (even more unstable than more idealized rings studied earlier), while in reality they appear able to survive" [*Katsman et al.*, 2003].

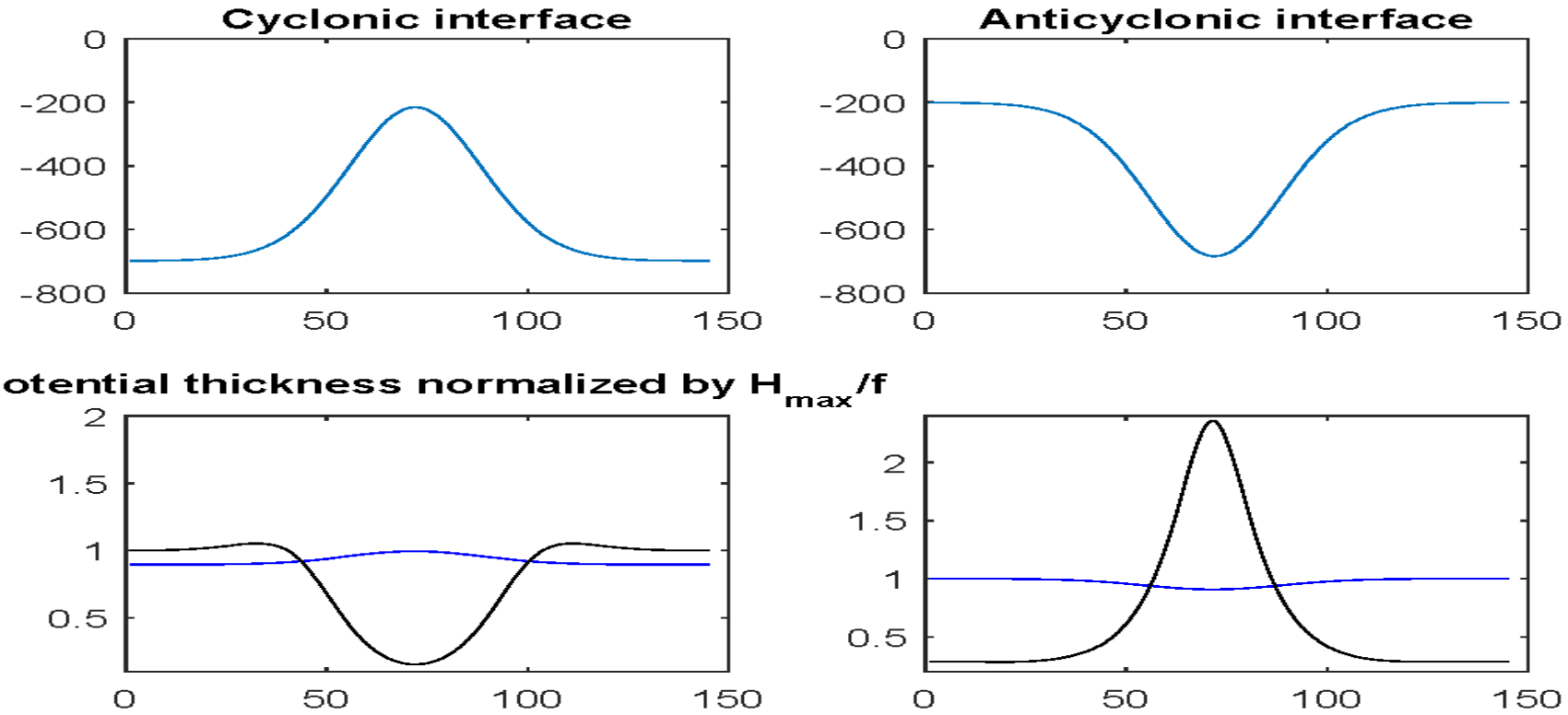

The vortex parameters and stratification were chosen to be consistent with famous examples of cold-core ring Bob [*Olson*, 1980] used for linear stability study by *Katsman et al.* [2003]. The Coriolis parameter $f = 0.83 \cdot 10^{-4}$ s^{-1} at 34.5 N, the maximum velocity $V_m \approx 1.4$ m/s at $r_c \approx 56$ km, so that $\Omega_0 \approx 0.35f$ in (19) gives $\Pi_1(0) \approx -9$ m^2/s^2, which must be consistent with maximum interface deviations: $\Pi_1(0) = g'_1 Z(0,\xi_1) + g'_2 Z(0,\xi_2)$. Choosing $\xi_1 = 700$ m and $\xi_2 = 1600$ m where observed $Z(0,\xi_1) \approx -500$ m, $Z(0,\xi_2) \approx -350$ m (Figure 1b), we prescribe $g'_1 = 0.015$ m/s^2 and $\gamma = 5$ that gives $L_1 \approx 39$ km and $R \approx 1.44$. The mean ocean depth in this region $H_1 + H_2 + H_B = 4.6$ km, so for the 3L setup $H_1 = 700$ m, $H_2 = 900$ m, and $H_B = 3000$ m, while for the equivalent 2L configuration $H_1 = 700$ m and $H_B = 3900$ m.

The depth of marginal stability for Gaussian cyclonic ring of such size would correspond to 7 km in the 2L model [*Benilov and Flanagan*, 2008]. Therefore, for our smaller depth, the vortex is unstable and strongly elongates until $T = 105$ days (Figure 4a) when the perturbation amplitude reaches the maximum (Figure 3). In the lower layer

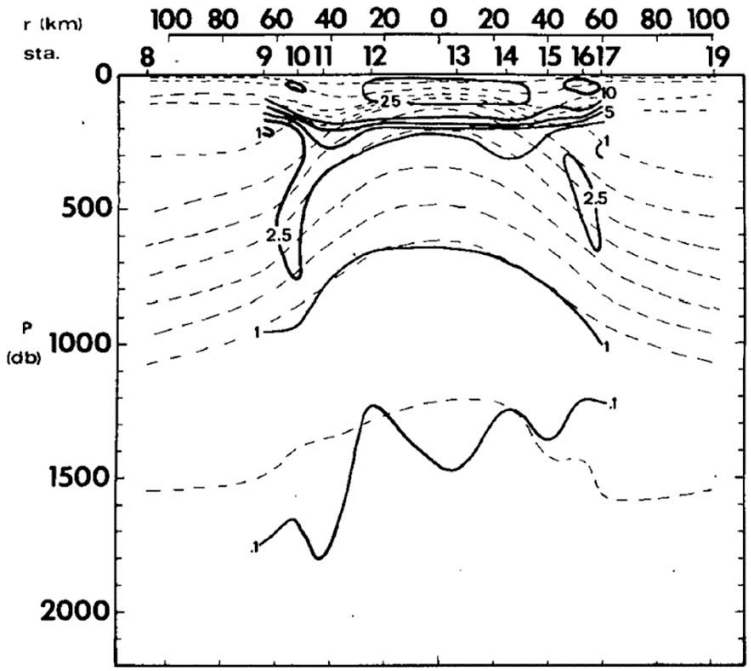

(a)

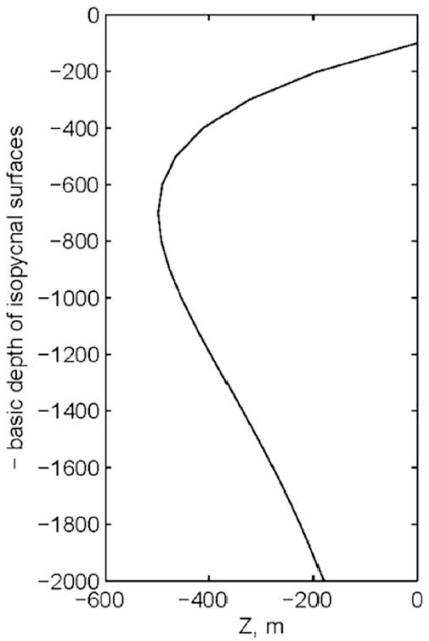

(b)

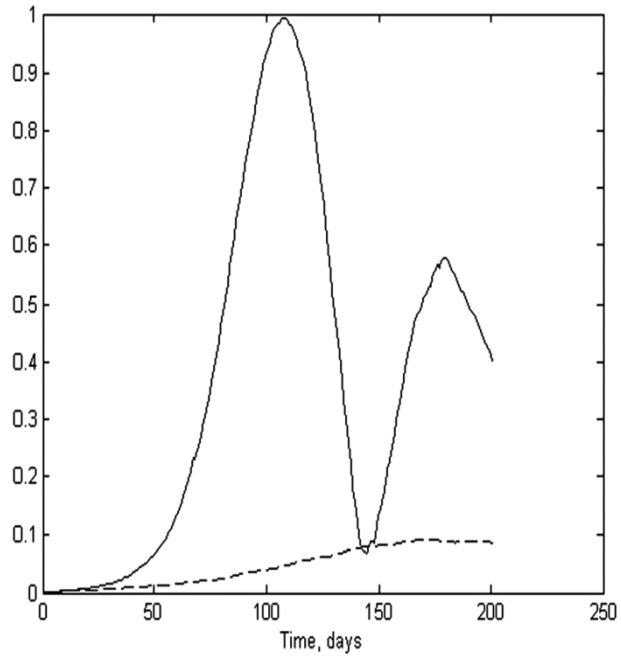

Figure 3. The time evolution of the perturbation amplitude for the 2L model (solid line) and 3L model (dashed line).

e 1. (a) The potential vorticity (solid contours) superimposed by the potential density field (dashed lines) for ring Bob of Figure 7a by *Olson* [1980]). (b) Isopycnal displacement $Z(0,\xi)$ at the cyclone center.

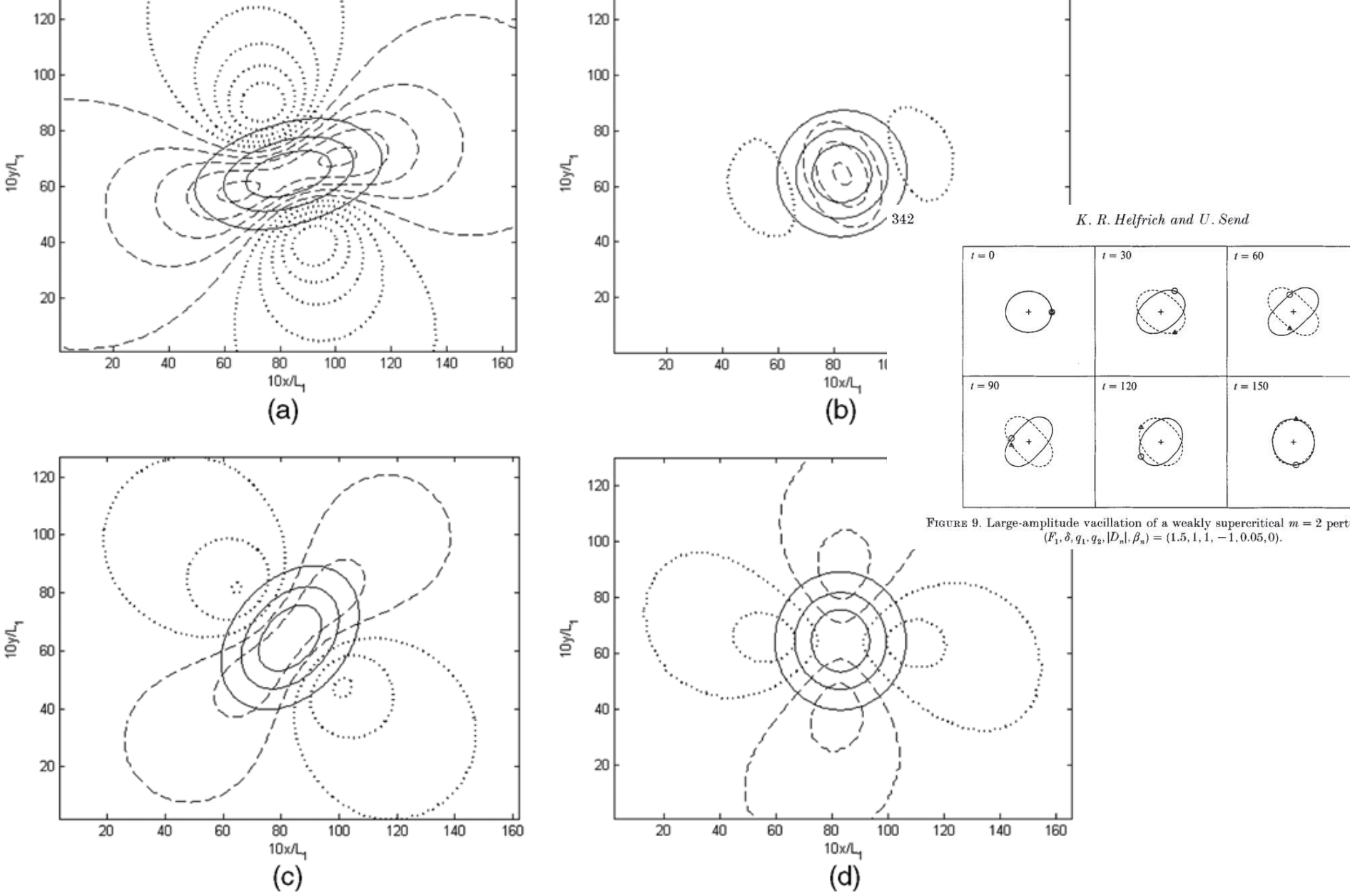

FIGURE 9. Large-amplitude vacillation of a weakly supercritical $m = 2$ pertu
$(F_1, \delta, q_1, q_2, |D_n|, \beta_n) = (1.5, 1, 1, -1, 0.05, 0)$.

Figure 4. Contours of the upper layer pressure (solid line) and the lower layer pressure (cyclonic, dashed line; anticyclonic, dotted line) for the 2L model at (a) $T = 105$ days, (b) $T = 145$ days, (c) $T = 180$ days, and (d) for the 3L model at $T = 180$ days.

WHY COLD CORE RINGS LOOK STABLE

Geophys. Res. Lett, 2015, v. 42

- A middle layer with uniform PV reduces the growth rate of baroclinic instability of circular compensated vortices in contrast to 2L models
- Weakly supercritical compensated eddies equilibrate in carousel multipole structures with slightly elongated upper core balanced by a self-induced strain by the deep partners.
- Medium supercritical eddies evolve towards long-lived corotating tripolar states with pulsating partners similar to 2D tripoles
- What is the bifurcation structure of eddies on the way to break into baroclinic dipoles found in the lab and model simulations?

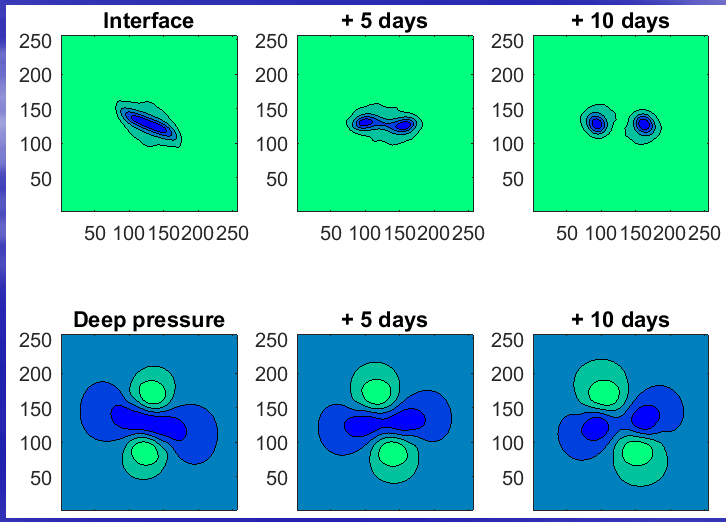

Warm core ring (Ro = 1/6, R = 6/7) in 3L and 2L models

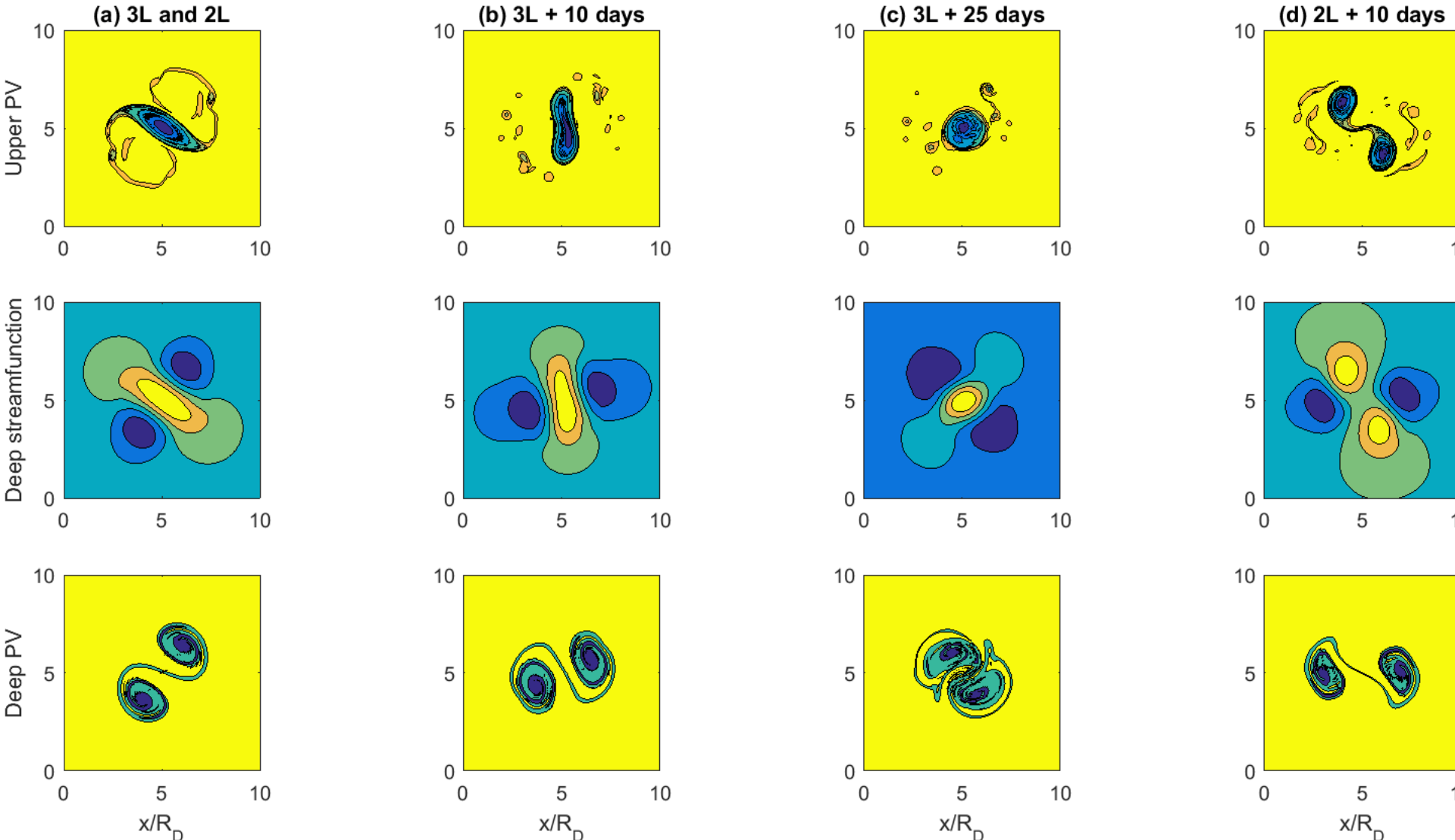

XAVIER CARTON† AND BERNARD LEGRAS‡

J. Fluid Mech. (1994), *vol.* 267, *pp.* 53–82

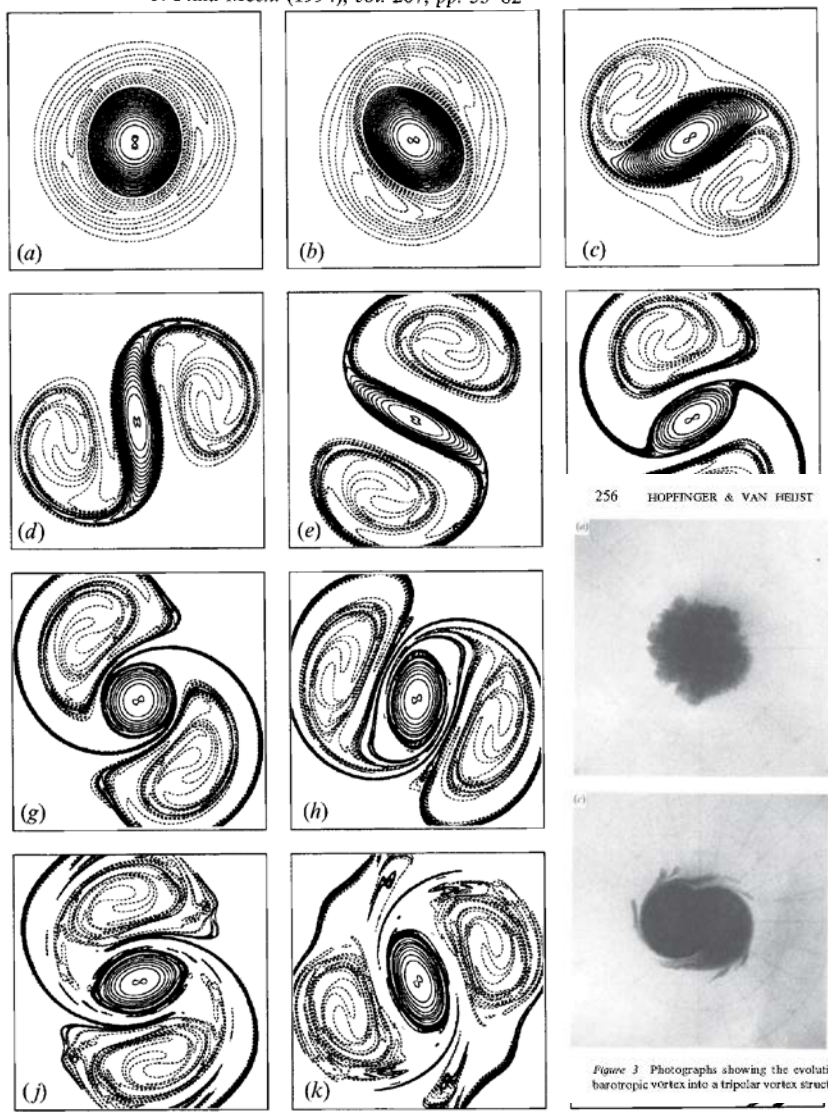

FIGURE 1. Vorticity maps from the 512^2 experiment at various times. Contour interval 0.05. Solid contours for positive vorticity and dashed contours for negative vorticity. The frame is centered and shows $\frac{11}{16} \times \frac{11}{16}$ of the periodic $2\pi \times 2\pi$ box. (*a*) $t = 30$ (2.3τ); (*b*) $t = 40$ (3.07τ); (*c*) $t = 55$ (4.22τ); (*d*) $t = 70$ (5.37τ); (*e*) $t = 85$ (6.52τ); (*f*) $t = 100$ (7.67τ); (*g*) $t = 107$ (8.21τ); (*h*) $t = 120$ (9.21τ); (*i*) $t = 140$ (10.74τ); (*j*) $t = 160$ (12.28τ); (*k*) $t = 195$ (14.97τ) and (*l*) $t = 230$ (17.65τ). Figure 8 shows the vorticity profile along the section.

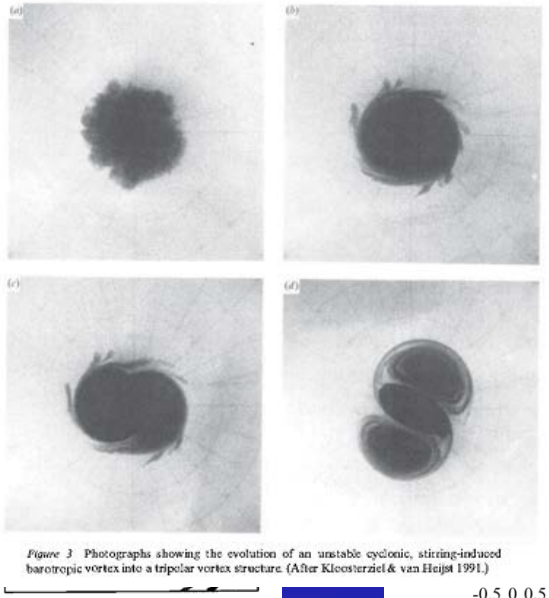

Figure 3. Photographs showing the evolution of an unstable cyclonic, stirring-induced barotropic vortex into a tripolar vortex structure. (After Kloosterziel & van Heijst 1991.)

J. Fluid Mech. (2000), *vol.* 423, *pp.* 127–154. Printed in the United Kingdom

Finite-core hetons: stability and interactions

By M. A. SOKOLOVSKIY[1] AND J. VERRON[2]

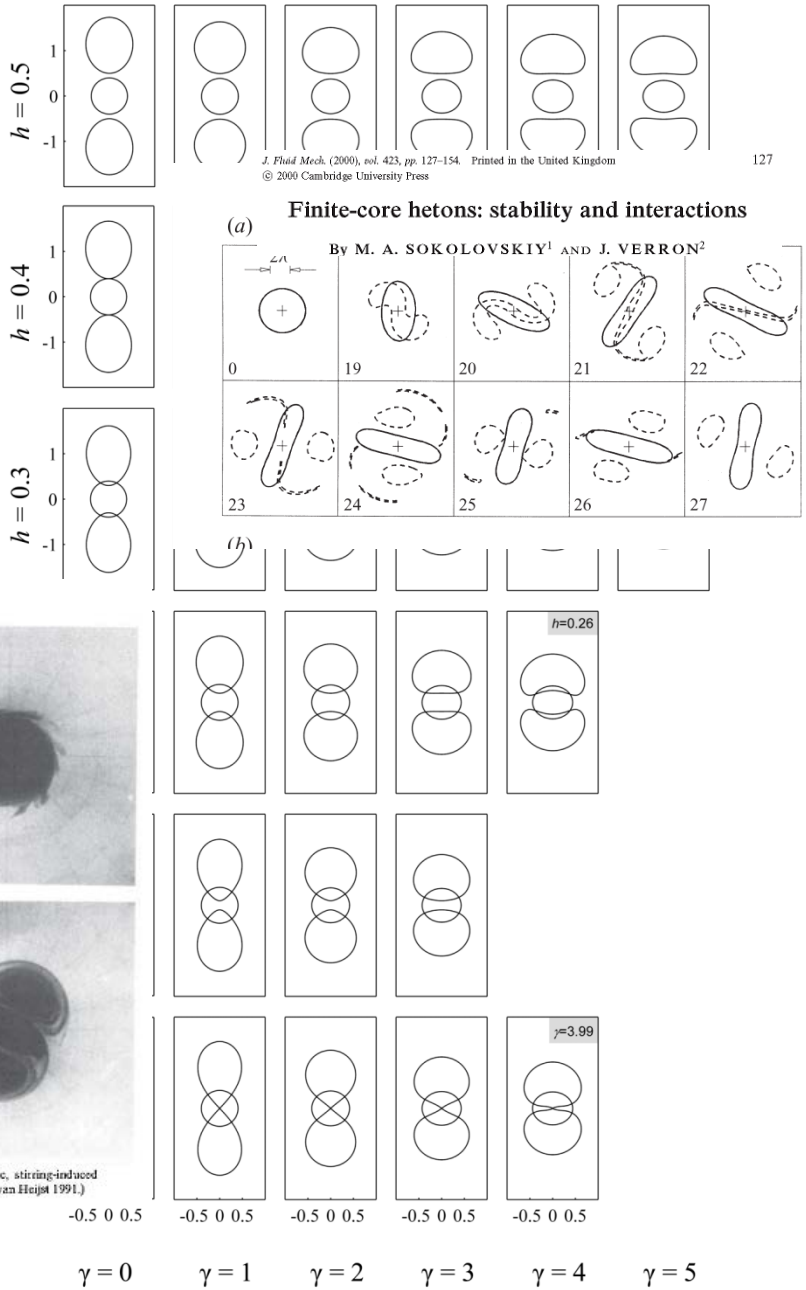

FIG. 3. Shapes of the tripole solutions computed at different combinations of parameters γ and h.

Upper Vorticity

Upper PT $H/(1+\zeta/f)$

Deep PT Anomaly

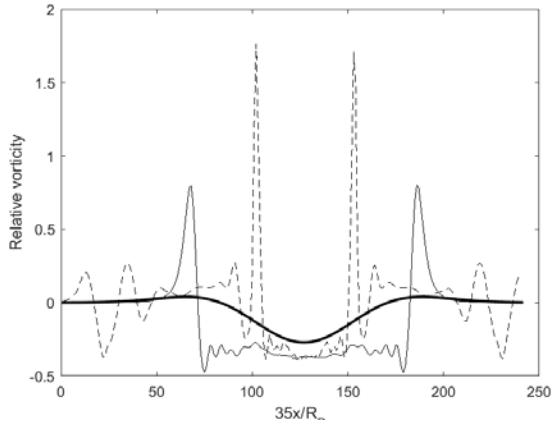

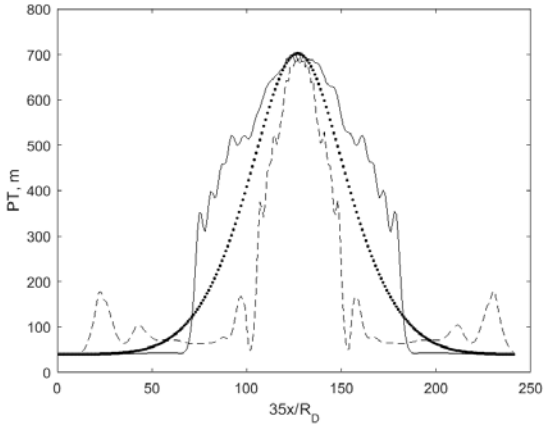

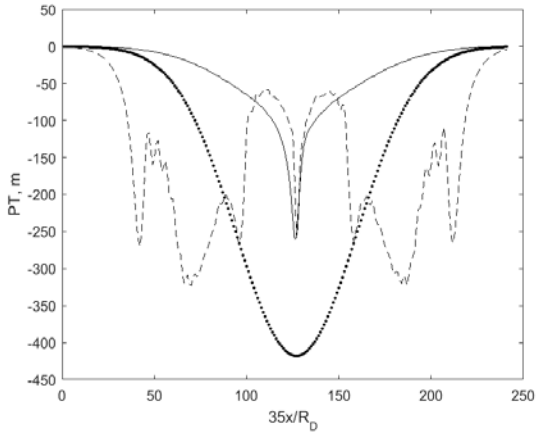

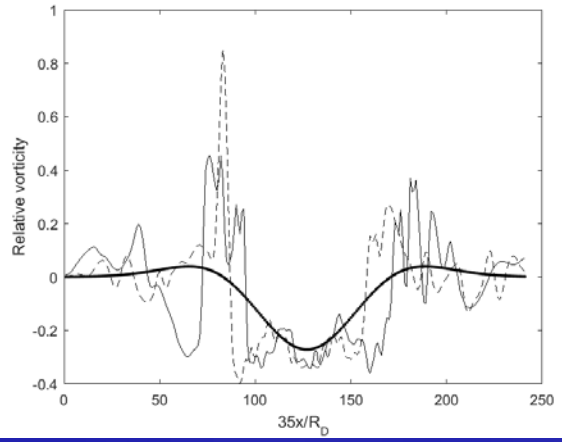

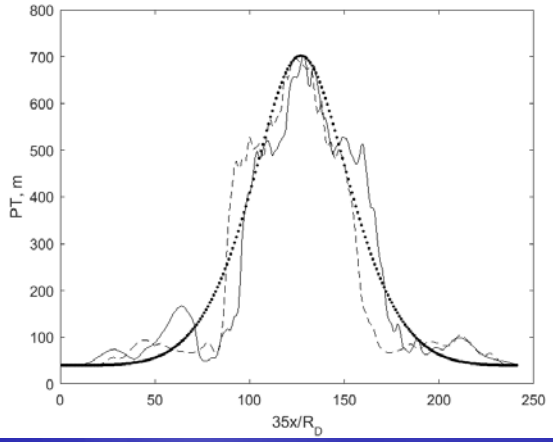

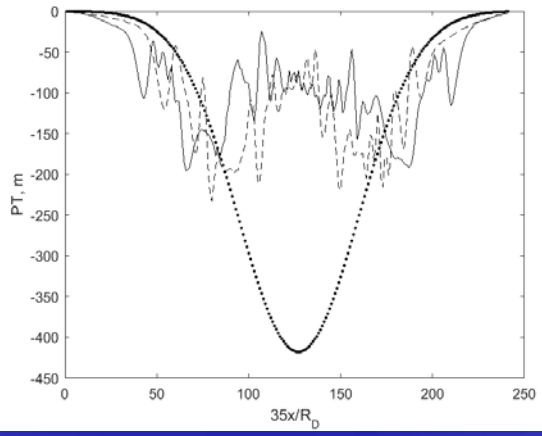

distances (and is identical with the interaction energy of M geostrophic point vortices)

$$H_C = -\sum_{k=1}^{M}\sum_{\alpha\neq k}^{M}\frac{Q_k Q_\alpha}{2}G(R_{k\alpha}),$$

and H_I which represents the second-order correction due to finite size

$$H_I = -\sum_{k=1}^{M}\sum_{\alpha\neq k}^{M}\frac{Q_k Q_\alpha}{4}\Omega_{k\alpha}\left[J_k\left(\lambda_k+\frac{1}{\lambda_k}\right)+J_\alpha\left(\lambda_\alpha+\frac{1}{\lambda_\alpha}\right)\right]$$

$$+\sum_{k=1}^{M}\sum_{\alpha\neq k}^{M}\frac{Q_k Q_\alpha}{4}\Upsilon_{k\alpha}\left[J_k\left(\lambda_k-\frac{1}{\lambda_k}\right)\cos(2\theta_{k\alpha}-2\phi_k)+J_\alpha\left(\lambda_\alpha-\frac{1}{\lambda_\alpha}\right)\cos(2\theta_{k\alpha}-2\phi_\alpha)\right]. \quad \text{(A 53)}$$

The first part of H_I is defined by the induced rotational frequency Ω while the other parts of H_I are defined by the strain rate Υ. In two dimensions the first part of H_I vanishes because $\Omega = 0$, so that (A 52)–(A 53) correspond to expressions (28) in the paper by Melander *et al.* (1986).

From (A 52)–(A 53) in agreement $G = \frac{1}{4\pi}\ln 2\rho = \frac{1}{2\pi}\ln r, \quad \hat{G} = \Upsilon = \frac{1}{4\pi\rho} = \frac{1}{2\pi r^2}, \quad \Omega = 0.$

$$Q_k\dot{Y}_k = -\partial_{X_k}(H_C+H_I), \quad Q_k\dot{X}_k = \partial_{Y_k}(H_C+H_I)$$

(similar to the Hamiltonian form of the point-vortex model).

$$\dot{\lambda}_k = 2\lambda_k\sum_{\alpha\neq k}^{M}Q_\alpha\Upsilon_{k\alpha}\sin(2\theta_{k\alpha}-2\phi_k),$$

$$\dot{\phi}_k = \dot{\phi}_k^{(i)} + \sum_{\alpha\neq k}^{M}Q_\alpha\left(\Omega_{k\alpha}-\frac{\lambda_k^2+1}{\lambda_k^2-1}\Upsilon_{k\alpha}\cos(2\theta_{k\alpha}-2\phi_k)\right),$$

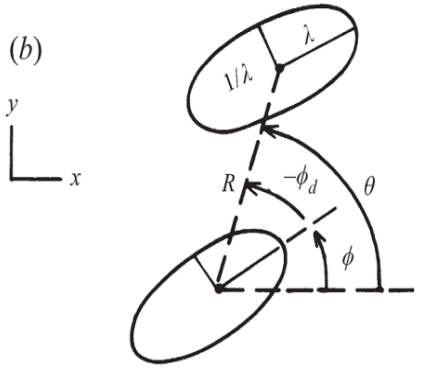

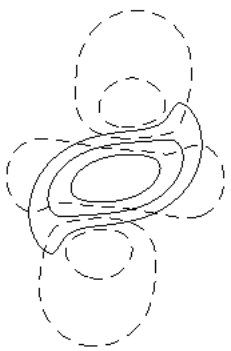

SELF-ELONGATION and SELF-INTENSIFICATION

Geophys. Res. Lett, 2016, submitted

- The upper core elongation is self-induced by the strain in the deep partners rotating with proper phase
- Equilibrated tripolar state is possible when the elongated upper core and deep partners stay in perpendicular directions
- Deep corotation leads to self-intensification of vortex flow in the upper core where the flow is approaching nearly solid-body rotation
- Further break into baroclinic dipolar couples (hetons) remains enigmatic being sensitive to model details.

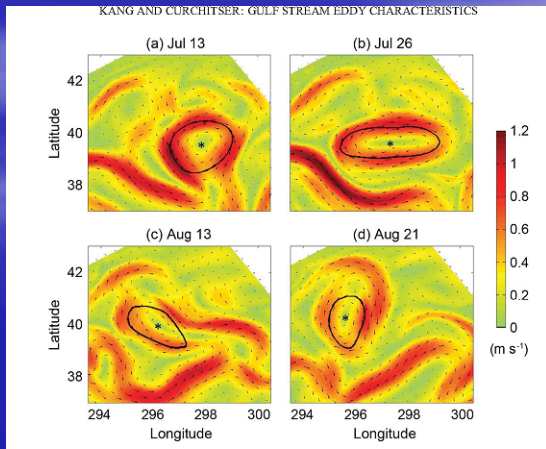

Figure 4. Evolution of an anticyclonic eddy in the summer 2000. Star indicates the eddy center, c
represents the amplitude of surface velocity, and vectors are plotted every five grid points. The ch
black lines denotes contours of $OW_0 = -0.2\sigma_{ow}$.

C. R. Acad. Sci. Paris, t. 313, Série II, p. 737-742, 1991

Mécanique des fluides/*Fluid Mechanics*

The enigmatic merging conditions of two-layer baroclinic vortices

Jacques VERRON and Emil J. HOPFINGER

Abstract – The influence of stratification on geostrophic vortex merging is investigated by using numerical simulations and the results of laboratory experiments.

Coalescence énigmatique de tourbillons baroclines en milieu bi-couche

Résumé – *Nous examinons le rôle de la stratification sur le contrôle de la coalescence de tourbillons géostrophiques à l'aide de simulations numériques et de résultats d'expériences de laboratoire.*

Version française abrégée – La coalescence des tourbillons est un mécanisme élémentaire de la dynamique de la turbulence géostrophique. En particulier, l'étude de l'interaction de deux tourbillons identiques dans un milieu stratifié à deux couches est le prototype le plus simple qui permette d'appréhender l'effet de la stratification sur la coalescence. A cet égard, les premières investigations de Verron et coll. [7] ont mis en évidence le rôle crucial des conditions initiales et expliqué les résultats contradictoires des travaux antérieurs de Griffiths et Hopfinger [2] et Polvani et coll. [6]. Plus spécifiquement, les tourbillons de vorticité potentielle (PVI, potential vorticity initialization) révèlent un comportement analogue à celui décrit par Polvani et coll. [6] dans lequel la stratification ne semble jouer aucun rôle. Au contraire, avec les tourbillons de vorticité relative (RVI, relative vorticity initialization) la stratification influence fortement la coalescence, conformément aux expériences de Griffiths et Hopfinger [2]. Dans ce dernier cas les simulations numériques de Verron et coll. [7] révèlent l'existence d'un pic dans la courbe de distance critique de coalescence d en fonction du paramètre de stratification λ (*voir* la figure 3, dans laquelle ces deux quantités λ et d sont adimensionalisées par le rayon R des tourbillons initiaux) qui traduit une forte sélectivité d'échelle dans le processus de coalescence.

Jets and Eddies in the Northwest Corner

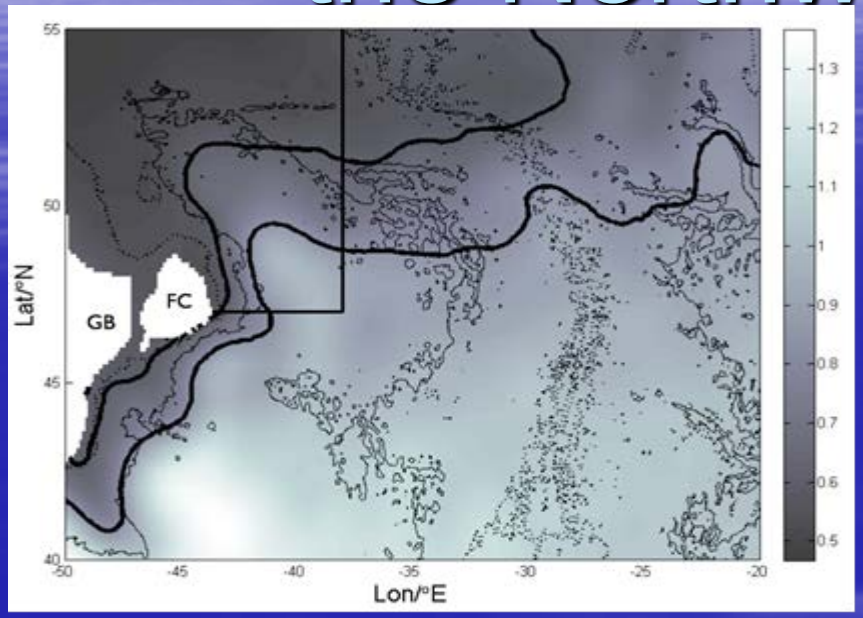

Mean MODAS sea surface height with elevation scale on the right in meters. The inshore edge of the NAC and SPF is indicated by a dynamic height contour at 0.6 m while the contour at 0.85 m runs along the principal baroclinic flow. Close together along the NAC they separate just south of the NWC. FC = Flemish Cap, GB = Grand Banks. 2000 and 4000 m isobaths shown. (From Woityra and Rossby, 2008.)

The North Atlantic Current (NAC) travels northward east of the Grand Banks until approximately 50°N where it makes a sharp turn to the east.

Previous analysis of sea level variability in this region, known as the Northwest Corner, showed a quasi-regular production of anticyclonic eddies playing an important role in the air-sea heat exchange.

Supported by NSF OCE-1027573

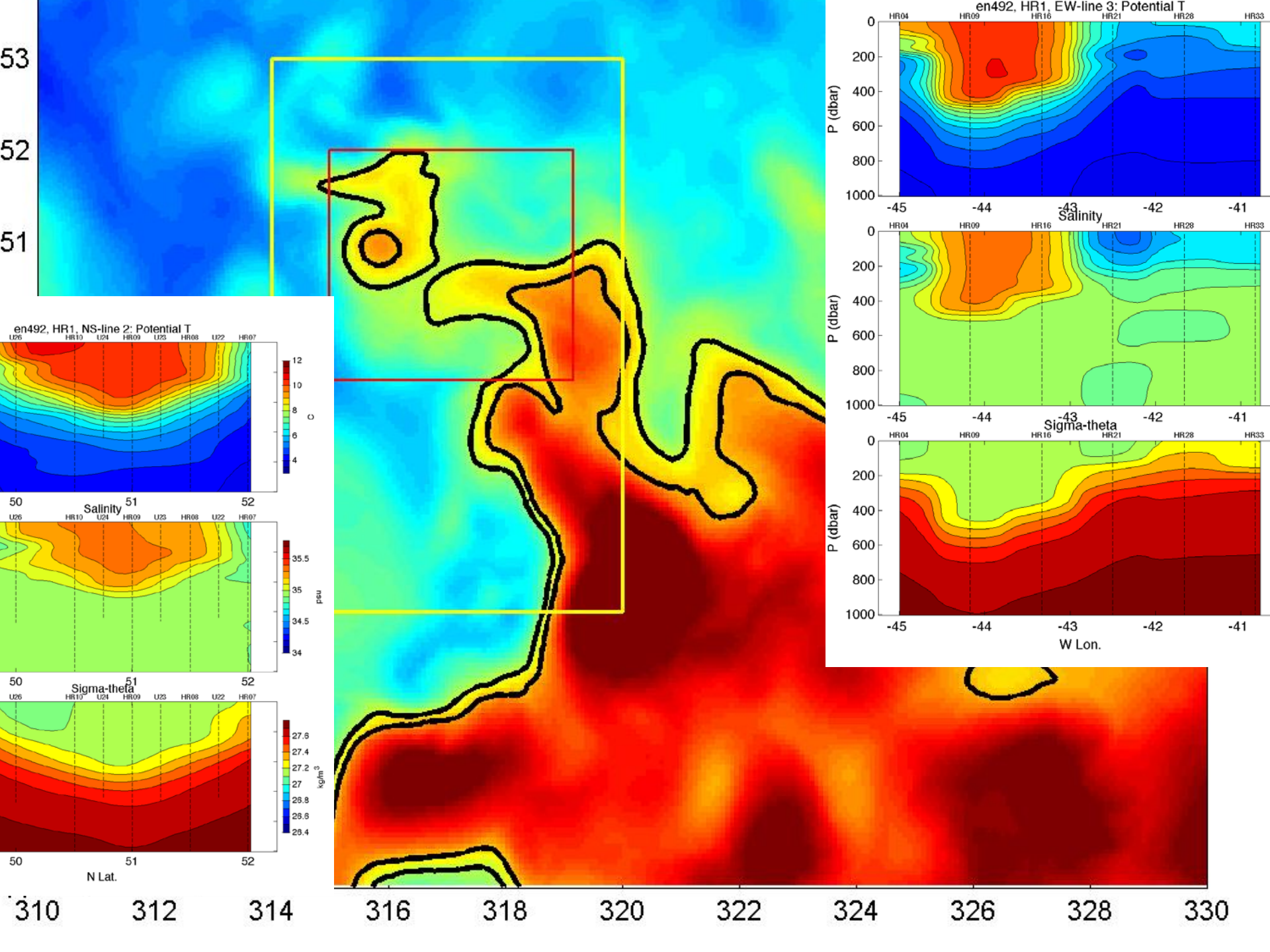
53
52
51
en492, HR1, NS-line 2: Potential T
U26 HR10 U24 HR09 U23 HR08 U22 HR07
12
10
8
6
4
C
50
51
52
Salinity
35.5
35
34.5
34
psu
Sigma-theta
27.6
27.4
27.2
27
26.8
26.6
26.4
kg/m3
N Lat.
en492, HR1, EW-line 3: Potential T
HR04 HR09 HR16 HR21 HR28 HR33
P (dbar)
0
200
400
600
800
1000
-45
-44
-43
-42
-41
Salinity
Sigma-theta
W Lon.
310
312
314
316
318
320
322
324
326
328
330

Vertical section of meridional velocity across the eddy and deep velocity field (HYCOM)

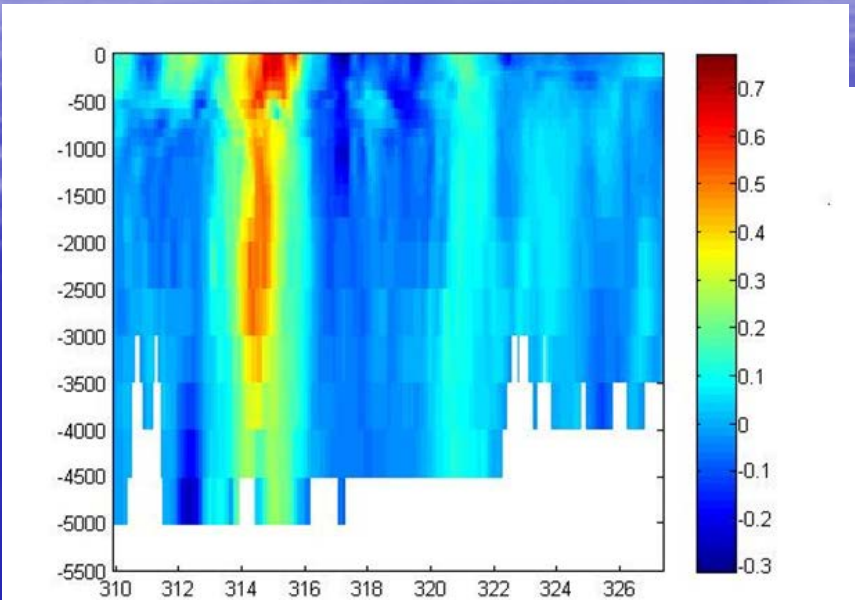

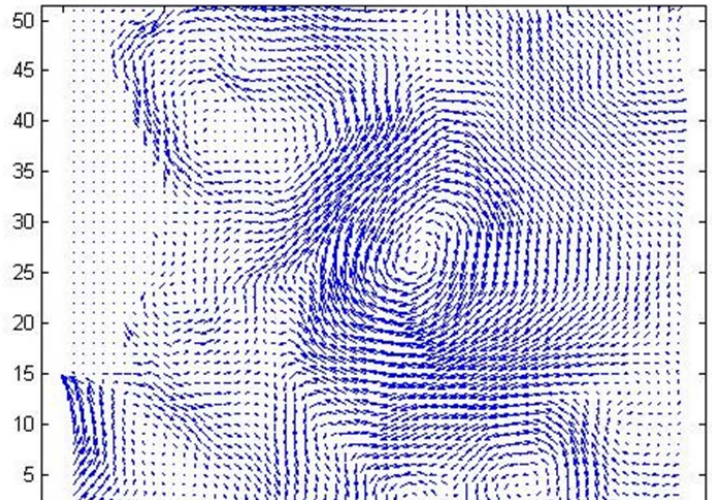

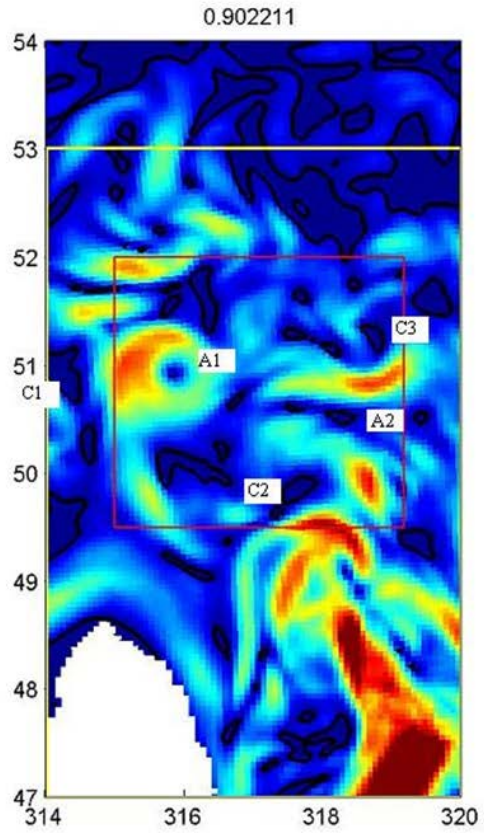

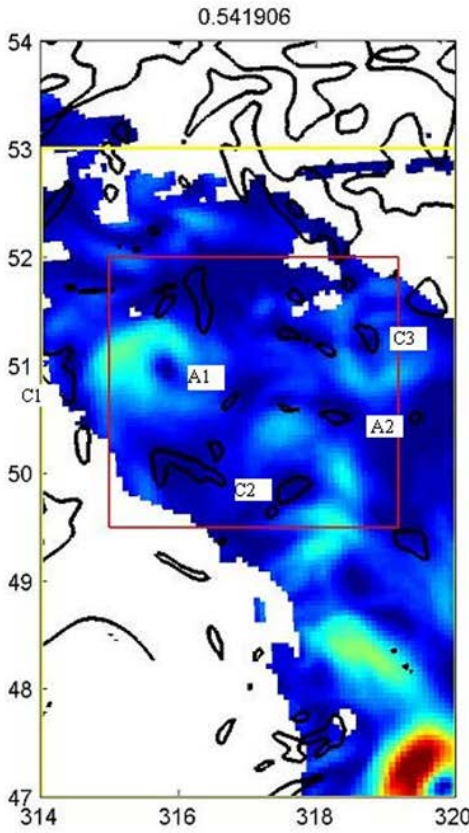

$$\frac{\partial \nabla^2 \psi}{\partial t} = \left(u - \frac{\partial \psi}{\partial s} + a\frac{\partial \kappa}{\partial s}\right)\frac{f}{H_2}\frac{\partial h}{\partial n} \approx -f^2 v(n)\frac{a}{g' H_2}\frac{\partial \kappa}{\partial s}, \tag{12}$$

where the midjet displacement is assumed to be proportional to the normal velocity (9) while $\frac{\partial \psi}{\partial s} \approx u$ across the jet,

$$\frac{\partial \theta}{\partial t} = a\frac{\partial^3 \theta}{\partial s^3} + \frac{\partial u}{\partial s}, \quad \text{or} \quad \frac{\partial \kappa}{\partial t} - a\frac{\partial^3 \kappa}{\partial s^3} = \frac{\partial^2 u}{\partial s^2}. \tag{13}$$

The amplification of meanders coupled with deep eddies is represented here by clear physical mechanisms: the generation of deep flow vorticity is caused by sideways displacements of the jet relative to the fluid in lower layer, which change the interface depth. This displacement is driven by variations of jet curvature (12) and coupled with evolution of jet curvature due to variations of deep crossjet velocity (13).

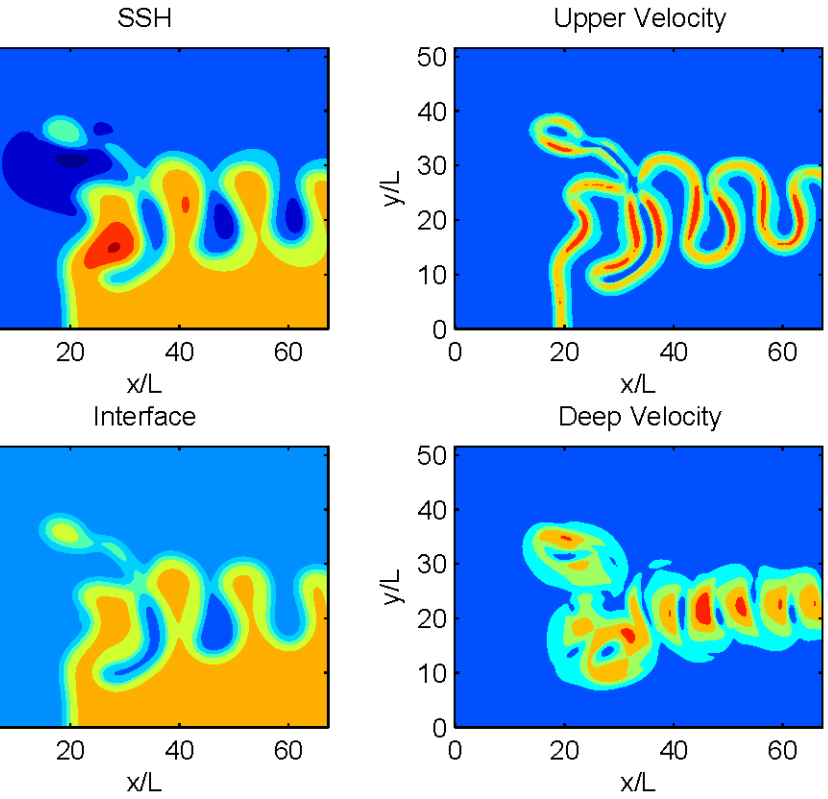

Generalized thin jet theory (DSR 2015)

Journal of Marine Research, 70, 719–747, 2012

Evidence of Vertical Coupling between the Kuroshio Extension and Topographically Controlled Deep Eddies

by Andrew D. Greene[1,2,3], D. Randolph Watts[4], Georgi G. Sutyrin[4] and Hideharu Sasaki[5]

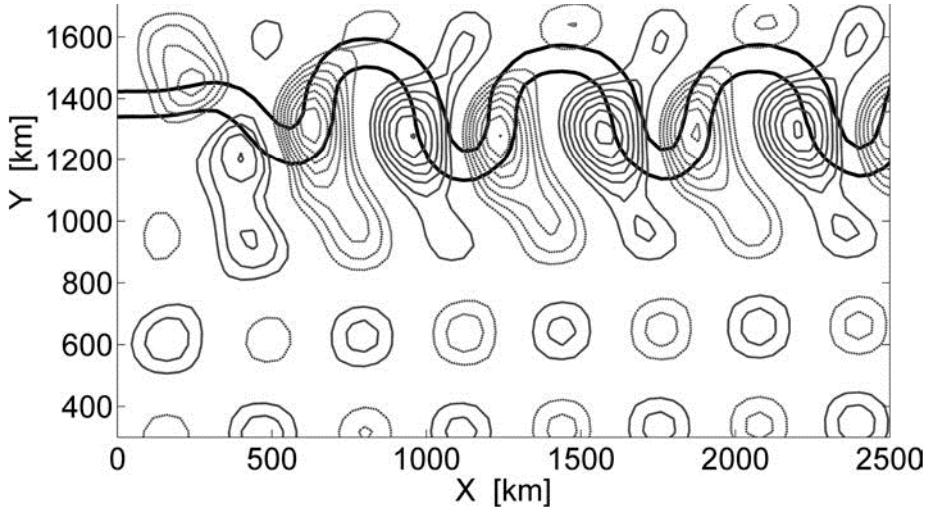

Figure 13. Upper and deep streamfunction fields from numerical model. Black bold lines denote the upper-ocean jet. Solid (dashed) gray contour lines represent the anticyclonic (cyclonic) portion of the topographic wave field. The contour interval for the deep field is .025 dbar. The top and bottom rows show the interaction at elapsed time $t = 0$ and 30 days, respectively. Initially the upper ocean jet was straight and during the interaction with barotropic TRWs the jet developed steep meander crests and troughs and the TRW amplitude intensified.